

Directional in-plane tunneling in oxygen-deficient $\text{YBa}_2\text{Cu}_3\text{O}_{6.6}/\text{YBa}_2\text{Cu}_{2.55}\text{Fe}_{0.45}\text{O}_y/\text{YBa}_2\text{Cu}_3\text{O}_{6.6}$ edge junctions

O. Neshet and G. Koren

Department of Physics, Technion-Israel Institute of Technology, Haifa, 32000, Israel

(Received 8 July 1999)

In-plane tunneling measurements of superconductor-insulator-superconductor (SIS)-type oxygen-deficient edge junctions made of $\text{YBa}_2\text{Cu}_3\text{O}_{6.6}$ as the superconductor and $\text{YBa}_2\text{Cu}_{2.55}\text{Fe}_{0.45}\text{O}_y$ as the barrier are reported. Two types of junctions were prepared in which transport is either along the (100) or the (110) direction. The dynamic conductance dI/dV shows a gaplike structure in the (100) junctions, while a zero-bias peak is observed in the (110) junctions. At energies below $\sim 2.5\Delta_0$ the results were found to be consistent with the Blonder, Tinkham, and Klapwijk model, extended by Tanaka and Kashiwaya to the case of $d_{x^2-y^2}$ -wave superconductivity. At higher energies the behavior of the dynamic conductance is explained as due to a self-heating effect inside the junction. [S0163-1829(99)04745-1]

In the past few years there has been an extensive effort to make tunneling measurements with $\text{YBa}_2\text{Cu}_3\text{O}_{7-\delta}$ (YBCO), in order to find the density of states, and to clarify the question of the symmetry of the pair potential in this material. Results of many tunneling experiments seem to show a predominant $d_{x^2-y^2}$ -wave symmetry of the pair potential. This leads to a change of sign in the phase of the order parameter each time the (110) or $(1\bar{1}0)$ directions are crossed. Theoretical studies of tunneling spectra based on the Blonder, Tinkham, and Klapwijk (BTK) model for $d_{x^2-y^2}$ -wave superconductors predict a gap structure along the principal (100) and (010) axes, while a zero-bias conductance peak (ZBCP) caused by Andreev-bound states on the surface is expected along the (110) and $(1\bar{1}0)$ directions.¹⁻³ In order to check these predictions, directional tunneling measurements in the a - b plane were made between normal metals and YBCO using scanning tunnel microscopy (STM), and point-contact junctions.^{4,5} The conductance results of these measurements show the expected spectra of a superconductor with a predominant $d_{x^2-y^2}$ -wave order parameter. In these experiments there is no clear separation between the various transport directions. For instance, the STM measurements show a strong ZBCP in the (100) direction, and a weak gap structure in the (110) direction that indicates mixed contributions to the conductivity from various directions. Tunneling experiments in planar SIS junctions made of thin films had also been done, with the transport current along either the c axis,^{6,7} or the a - b plane.^{8,9} The dynamic conductance of these junctions show similar tunneling spectra in both directions, possibly because of the rough interfaces in these junctions.

To overcome these problems we decided to study tunneling junctions with an edge geometry in which the electrodes are made of oxygen-deficient $\text{YBa}_2\text{Cu}_3\text{O}_{6.6}$. These junctions have a larger coherence length ξ_0 , and smooth flat interfaces that can be made at any desired direction with respect to the crystalline axes in the a - b plane. Recently, we showed that these junctions can have either superconductor-normal-superconductor (SNS) or SIS properties, depending on the specific junction parameters used in their preparation pro-

cess, such as the barrier thickness and the edge angle.^{10,11} In the SNS-type edge junctions we were able to measure geometrical resonances resulting from interference of quasiparticles in the normal N barrier (McMillan-Rowell oscillations),¹⁰ and in the superconducting S electrode (Tomashch oscillations).¹¹ The ability to observe these interference effects indicates that the interfaces in our junctions are quite smooth and flat. In this study we focus on SIS-type edge junctions, with interfaces normal to either the (100) or the (110) directions. The measured dynamic conductance dI/dV of the (100) oriented junctions showed a gaplike structure, while a ZBCP was observed in the (110) oriented junctions. These results are consistent with the BTK formalism with a predominant $d_{x^2-y^2}$ -wave symmetry of the order parameter at energies below $\sim 2.5\Delta_0$. At higher energies however, a monotonous decrease of the dynamic conductance was observed, which resulted from self-heating effects in the junctions at the higher bias currents.

Oxygen-deficient edge junctions with $\text{YBa}_2\text{Cu}_3\text{O}_{6.6}$ ($T_c = 60$ K) as the superconductor, and $\text{YBa}_2\text{Cu}_{2.55}\text{Fe}_{0.45}\text{O}_y$ as the barrier were prepared, as described in detail before.¹¹ A schematic diagram of the junction is shown in Fig. 1. Briefly, the base electrode and the insulator were deposited onto a (100) SrTiO_3 (STO) wafer of 1×1 cm² area by laser ablation deposition. Then using a waterless deep UV photolithographic process, we prepared the edge by Ar ion milling at an angle $\alpha = 36^\circ$, with excess milling into the substrate down to $d_{\text{sub}} = 70$ nm. After this, a second deposition run

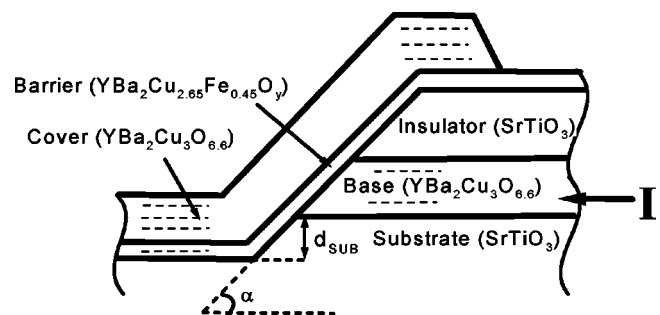


FIG. 1. A schematic diagram of an edge junction.

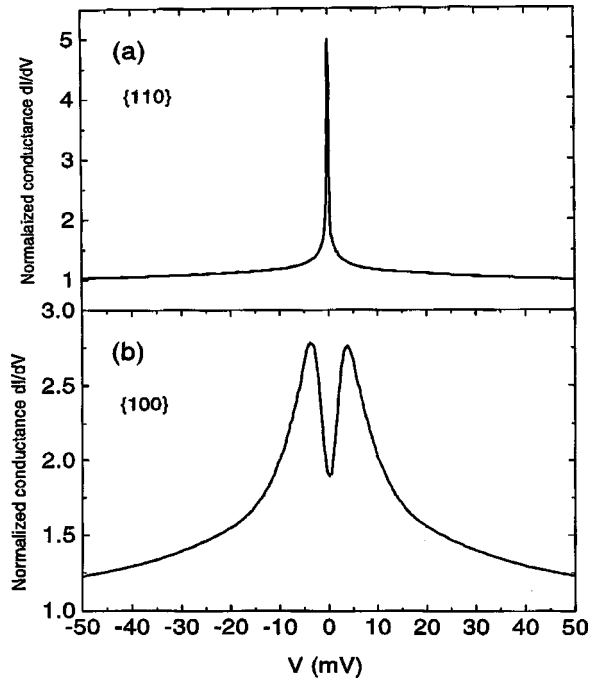


FIG. 2. Dynamic conductance data dI/dV of oxygen-deficient $\text{YBa}_2\text{Cu}_3\text{O}_{6.6}/\text{YBa}_2\text{Cu}_{2.55}\text{Fe}_{0.45}\text{O}_y/\text{YBa}_2\text{Cu}_3\text{O}_{6.6}$ edge junction with interfaces perpendicular to the (110) direction (a), and the (100) direction (b).

was carried out, in which a barrier, a cover electrode, and gold contact layers were prepared. The sample was then cooled down in flowing oxygen at 40 mTorr to obtain the 60 K phase. Finally, the sample was patterned into 10 junctions, each of 5 μm width. The thicknesses of the base, barrier, and cover layers were 70, 20–30, and 70 nm, respectively.

The dynamic conductance dI/dV of the junctions at 4.2 K was measured by *direct differentiation* of the I - V curves, using ac modulation dI , and a lock-in amplifier for the detection of dV . Typical results of the measured dynamic conductance in our junctions are shown in Fig. 2. In Fig. 2(a) the interface of the junction is normal to the (110) direction, while in Fig. 2(b) the interface of the junction is normal to the (100) direction. One can see that the conductance in Fig. 2(a) has a clear ZBCP, while in Fig. 2(b) it has a gaplike structure with maxima at energies of about ± 5 meV. Spectra similar to those of Fig. 2 were observed before in STM experiments, where the tunneling conductance between a metallic tip and a YBCO single crystal was measured.^{4,5} However, unlike the previous results, the present data does not show mixing of orientations. Along the (100) direction there is only a gap structure without a ZBCP, and along the (110) direction we see the ZBCP without any gap structure. This results from the flatness of the interfaces in our junctions.

In order to analyze these results, we used the BTK formalism,⁹ which was extended to include $d_{x^2-y^2}$ -wave symmetry by Tanaka and Kashiwaya.^{2,3} In a $d_{x^2-y^2}$ -wave superconductor the density of states (DOS) near the interface is affected by Andreev scattering of electronlike quasiparticles and holelike quasiparticles. In this process the pair potential can change sign, thus an electronlike quasiparticle that is injected or reflected at the interface might feel a different

sign of the pair potential if the angle between the crystalline axes and the normal to the interface is not zero. As a result, zero-energy bound states can be formed near the interface, and give rise to a zero-bias peak in the conductivity. These ZBCP have maximum intensity when the transport is along the (110) direction of the nodes in the gap, and the angle between the principal axes of the superconductor and the normal to the interface is $\pi/4$. We calculated first $N(E)$ the DOS of the superconductor near the interface using the Tanaka and Kashiwaya model for the scattering processes described above. Then we used it to calculate the conductivity of the SIS junctions as follows:

$$\sigma = \frac{\sigma_{NN}}{e} \frac{d}{dV} \int_{-\infty}^{\infty} dE N(E) N(E-eV) [f(E-eV) - f(E)], \quad (1)$$

where σ_{NN} is the conductance of an NIN junction, and $f(E)$ is the Fermi-Dirac distribution function. σ_{NN} is given by

$$\frac{1}{\pi} \int_{-\pi/2}^{\pi/2} d\theta \frac{4 \cos^2 \theta}{4 \cos^2 \theta + Z^2},$$

where Z represents the barrier strength.¹ The exact expression for $N(E)$ is given by Eq. (52) in Ref. 3. In order to fit our results to Eq. (1), we had to use a lifetime broadening parameter Γ that was first introduced by Dynes, as an imaginary part added to the energy E .¹² The best fits to our data are shown by the dashed curves in Fig. 3. From these fits we obtained a barrier strength of $Z=1$, $\Delta_0=5$ meV, and a broadening ratio of $\Gamma/\Delta_0=0.3$. In Fig. 3(b) one can see that the calculated conductance above about 30 meV is constant, while in our measurements the conductance is decreasing monotonously with the bias voltage. We attribute this effect to self-heating in the junction, which is caused by the high bias current. In the next paragraph we shall elaborate on how this heating leads to a decay of σ versus V that affects our data. In fact, we shall have to multiply the calculated conductance by a factor of $[c/(c+V)]^{1.5}$, where c is an empirical parameter, and V is the bias voltage. But before doing that we note that in Fig. 3(a) at energies of 1–3 meV, and in Fig. 3(b), at energies of 10–25 meV the calculated conductance given by the dashed curves underestimates the experimental results. These discrepancies between the calculations and our experimental results seem to suggest that in our calculations we should have added an additional conducting channel in parallel to the original one, with conductivity σ_1 and pair potential Δ_1 that is larger than Δ_0 . Such a situation in which $\sigma = a\sigma_0(\Delta_0) + b\sigma_1(\Delta_1)$ where a and b are constants, can arise if we assume that in our junctions conduction occurs via two different kinds of parallel channels. A dominant one with oxygen-deficient electrodes and Δ_0 gap, and a subdominant one with locally well-oxygenated electrodes and Δ_1 gap. In the fits of our data we thus used $\Delta_0 = 5$ meV, $\Delta_1 = 20$ meV, $b/a = 1/6$, and included also the self-heating factor. The results of these fits are plotted by the solid curves in Fig. 3. Clearly, these fits are satisfactory, and in good agreement with the experimental data. We attribute the small value of $\Delta_0 = 5$ meV to the fact that the cover electrode, which grows on the inclined part of the edge with exposed a - b planes on the opposite side to the barrier, suf-

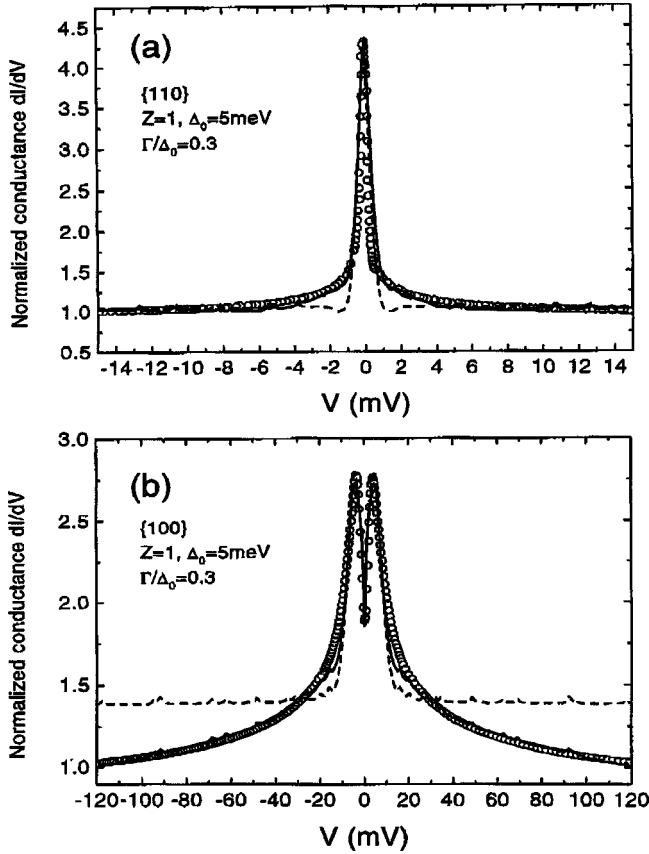


FIG. 3. Dynamic conductance data dI/dV of oxygen-deficient $\text{YBa}_2\text{Cu}_3\text{O}_{6.6}/\text{YBa}_2\text{Cu}_{2.55}\text{Fe}_{0.45}\text{O}_y/\text{YBa}_2\text{Cu}_3\text{O}_{6.6}$ edge junction with interfaces perpendicular to the (110) direction (a), and the (100) direction (b) (open circles). Best fits using the extended BTK model with a $d_{x^2-y^2}$ -wave symmetry of the order parameter (dashed lines), and with an additional component of $\Delta_1=20$ meV, and the self-heating effect (solid lines).

fers from defects and microcracks as was observed by others in many TEM studies.^{13–15} These defects can serve as channels for oxygen migration out of the YBCO layer, which reduces the gap parameter of the cover electrode near the active area of the junction. In order to understand the origin of the larger gap Δ_1 , and to demonstrate the self-heating effect in our junctions, we shall analyze next the dynamic conductance of another set of junctions that were prepared

without over milling into the substrate. Unlike the case of the previous junctions, in these junctions the active part of the cover electrode is protected, and has no exposed a - b planes that lead to the lower gap value Δ_0 .

A typical result of the dynamic conductance of a (100) oriented junction with $d_{sub}=0$ (see Fig. 1) is shown by the open circles in Fig. 4. One can see that a $d_{x^2-y^2}$ -wave symmetry is consistent with it below 50 meV, with $Z=1$, $\Delta_1=20$ meV, and $\Gamma/\Delta_1=0.3$. Therefore, when the a - b planes of the cover electrode are well protected, we see only the well-developed gap $\Delta_1=20$ meV. Above 50 meV the calculated conductance becomes constant, while our measured conductance is decreasing monotonically with the bias voltage. We attribute this behavior of the dynamic conductance, to thermal heating of the junction. The heat developed in the resistive part of the junction as a result of the current through it can be dissipated by conduction mainly via the YBCO electrodes. This is so because the electrodes have the largest contact area with the junction, and the largest heat conductance as compared to that of the STO substrate, and the ambient He gas. Therefore we can assume that to a first approximation, the heat conduction in the junction is one dimensional, and along the current path. This leads to a steady-state equation for the heat conduction in the junction at any given bias voltage V , which is given by

$$I(V)V = \frac{V^2}{dV/dI} = \frac{\Delta T \kappa A}{L}, \quad (2)$$

where V is the bias voltage on the junction, ΔT is the temperature gradient between the junction and the liquid-He bath ($\Delta T = T_{junction} - 4.2$ K), κ is the thermal conductance of YBCO [1.5 W/cm K (Refs. 16 and 17)], A is the cross-sectional area of the junction, and L is the length of the electrodes. At 50 mV the current is 5 mA, thus the electric power in the junction is 0.25 mW. In our junctions A is 5×10^{-9} cm², and L is 5 μ m. Substituting these parameters in Eq. (2), we obtain a temperature increase of $\Delta T=17$ K at 50 mV. We measured the dynamic conductance dI/dV of our junctions as a function of temperature, and found that above 50 meV, $dI/dV \sim (\Delta T)^{-n}$ at constant V (~ 75 mV), where n varies between 2 to 3. A typical result is shown in the inset to Fig. 4, where one can see that a ΔT of 17 K leads

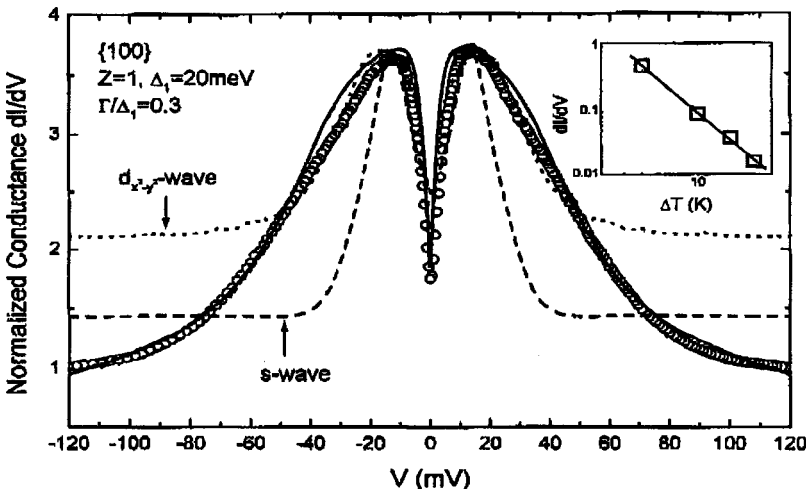


FIG. 4. Dynamic conductance data dI/dV of oxygen-deficient $\text{YBa}_2\text{Cu}_3\text{O}_{6.6}/\text{YBa}_2\text{Cu}_{2.55}\text{Fe}_{0.45}\text{O}_y/\text{YBa}_2\text{Cu}_3\text{O}_{6.6}$ edge junction with interfaces perpendicular to the (100) direction, and $d_{SUB}=0$ (open circles). Best fits according to the extended BTK model with s -wave symmetry (dashed line), $d_{x^2-y^2}$ -wave symmetry (dotted line), and with $d_{x^2-y^2}$ -wave symmetry and the self-heating effect (solid line). Inset: dI/dV at constant voltage as a function of the temperature difference between the junction and the bath at 4.2 K (ΔT) on a log-log scale.

to a significant reduction in the dynamic conductance dI/dV . Substituting the relation $dI/dV \propto (\Delta T)^{-n}$ in Eq. (2) yields

$$\frac{dI}{dV} \propto \left(\frac{dI}{dV} V^2 \right)^{-n}. \quad (3)$$

Assuming a power-law solution for Eq. (3) in the form of $dI/dV \propto (V)^m$, we find that $m = -2n/(1+n)$, and for $n=3$ one obtains $dI/dV \propto (V)^{-1.5}$. Thus the self-heating effect can be included in our calculations of the dynamic conductance by multiplying the conductance of Eq. (1) by the factor $[c/(c+V)]^{1.5}$, where c is a constant. Using this model and a pure $d_{x^2-y^2}$ -wave order parameter with $\Delta_1=20$ meV, we found that the best fit to our data is given by the solid curve in Fig. 4 ($c=35$ mV). From the solid curves in Figs. 3(b) and 4, one can see that the use of the self-heating effect is justified, as it describes well the behavior of dI/dV at higher bias voltages. We also checked the effect of possible additional s or is symmetry components in the order parameter up to 0.25 of Δ_1 , and found no significant changes in our fits.

Thus the present data does not support but also does not rule out either $d+s$ or $d+is$ symmetries of the order parameter.

In summary, we studied oxygen-deficient SIS-type edge junctions with $\text{YBa}_2\text{Cu}_3\text{O}_{6.6}$ electrodes. ZBCP was observed in the dynamic conductance of the (110) oriented junctions, while a gap structure was observed in the (100) oriented junctions. These results were found to be consistent with the extended BTK theory with a $d_{x^2-y^2}$ -wave symmetry of the order parameter. Our data supports two parallel conducting channels of the type $\sigma = a\sigma_0(\Delta_0) + b\sigma_1(\Delta_1)$, one with $\Delta_0 = 5$ meV and another one with $\Delta_1 = 20$ meV in one case, and a pure $\Delta = \Delta_1$ in another case. We also found that a self-heating effect caused by the electric power dissipated in our junctions, affects the measured dI/dV at high bias currents.

We wish to thank E. Polturak for useful discussions, and S. Hoida and M. Ayalon for technical assistance. This research was supported in part by the Heinrich Hertz Minerva Center for HTSC, the Israel Science Foundation, and the Fund for the Promotion of Research at the Technion.

-
- ¹G. E. Blonder, M. Tinkham, and T. M. Klapwijk, Phys. Rev. B **25**, 4515 (1982).
²Y. Tanaka and S. Kashiwaya, Phys. Rev. Lett. **74**, 3451 (1995).
³Y. Tanaka and S. Kashiwaya, Phys. Rev. B **53**, 9371 (1996).
⁴J. Y. T. Wei, N.-C. Yeh, D. F. Garrigus, and M. Strasik, Phys. Rev. Lett. **81**, 2542 (1998).
⁵L. Alff, H. Takashima, S. Kashiwaya, N. Terada, H. Ihara, Y. Tanaka, M. Koyanagi, and K. Kajimura, Phys. Rev. B **55**, 14 757 (1997).
⁶A. M. Cucolo, R. Di Leo, A. Nigro, P. Romano, F. Bobba, F. Bacca, and P. Prieto, Phys. Rev. Lett. **76**, 1920 (1996).
⁷K. A. Kouznetsov, A. G. Sun, B. Chen, A. S. Katz, S. R. Bahcall, J. Clarke, R. C. Dynes, D. A. Gajewski, S. H. Han, M. B. Maple, J. Giapintzakis, J.-T. Kim, and D. M. Ginsberg, Phys. Rev. Lett. **79**, 3050 (1997).
⁸M. Covington, M. Aprili, E. Paroanu, L. H. Greene, F. Xu, J. Zhu, and C. A. Mirkin, Phys. Rev. Lett. **79**, 277 (1997).
⁹D. Rcah and G. Deutscher, Physica C **263**, 218 (1996).
¹⁰O. Neshor and G. Koren, Phys. Rev. B **60**, 9287 (1999).
¹¹O. Neshor and G. Koren, Appl. Phys. Lett. **74**, 3392 (1999).
¹²R. C. Dynes, V. Narayanamurti, and J. P. Garno, Phys. Rev. Lett. **41**, 1509 (1978).
¹³C. L. Jia, B. Kabius, K. Urban, K. Herrman, G. J. Cui, J. Schubert, W. Zander, A. I. Braginski, and C. Heiden, Physica C **175**, 545 (1991).
¹⁴J. G. Wen, N. Kshizuka, C. Traeholt, H. W. Zandbergen, E. M. C. M. Reuvekamp, and H. Rogalla, Physica C **255**, 293 (1995).
¹⁵Y. Huang, K. L. Merkle, B. H. Moeckly, and K. Char, Physica C **314**, 36 (1999).
¹⁶K. Krishana, J. M. Harris, and N. P. Ong, Phys. Rev. Lett. **75**, 3529 (1995).
¹⁷B. Zeini, A. Freimuth, B. Buchner, R. Gross, A. P. Kampf, M. Klaser, and G. Muller-Vogt, Phys. Rev. Lett. **82**, 2175 (1999).